A comparative study of composite structures reinforced with carbon, glass or natural fibers

A comparative study of composite structures including carbon, glass and natural fibers

Salvatore Brischetto*

Abstract

This paper proposes a comparative study between different structures including fibre reinforced composite materials. Plates, cylinders, cylindrical and spherical shell panels in symmetric 0°/90°/0° and anti-symmetric 0°/90°/0°/90° configurations are analyzed considering carbon fiber, glass fiber and linoleum fiber reinforcements. A free vibration analysis is proposed for different materials, lamination sequences, vibration modes, half-wave numbers and thickness ratios. Such an analysis is conducted by means of an exact three-dimensional shell model which is valid for simply supported structures and cross-ply laminations. The employed model is based on a layer-wise approach and on three-dimensional shell equilibrium equations written in general orthogonal curvilinear coordinates. The proposed study confirms the well-known superiority of the carbon fiber reinforced composites. Linoleum fiber reinforced composites result comparable to glass fiber reinforced composites in the case of free vibration analysis. Therefore, similar frequencies are obtained for all the geometries, thickness ratios, laminations sequences, vibration modes and a large spectrum of half-wave numbers. This first partial conclusion needs further confirmations via static, buckling and fatigue analyses.

Keywords: fiber reinforced composites; carbon fibers; glass fibers; linoleum fibers; natural fibers; free vibration analysis; three-dimensional shell model.

*Corresponding author: Salvatore Brischetto, Department of Mechanical and Aerospace Engineering, Politecnico di Torino, corso Duca degli Abruzzi, 24, 10129 Torino, ITALY. tel: +39.011.090.6813, fax: +39.011.090.6899, e.mail: salvatore.brischetto@polito.it.

1 Introduction

The main improvements in future aircraft and spacecraft, such those discussed in Brischetto et al. (2016a) and Ferro et al. (2016), may depend on an increasing use of conventional and unconventional multilayered structures. One of these configurations is represented by carbon fiber reinforced laminates where the fiber orientation in each lamina and the stacking sequence of the layers can be chosen to achieve the desired strength and stiffness for a specific application [Brischetto (2014d)]. The use of composite structures, in particular those including carbon fibre reinforced composite materials, has grown in the last three decades. Today, carbon fiber reinforced composite materials have a great diffusion in different engineering fields. Such materials combine high performances with a relative low weight, and their study remains a cumbersome subject which concerns the delamination, damage and fracture analysis [Allix et al. (2010); Távara at al. (2010); Valisetty at al. (2010)], the computational structural model implementations [Baltacoglu and Civalek (2010); Brischetto (2014b); Brischetto (2014c); Hwu and Yu (2010); Rodríguez-Tembleque and Aliabadi (2014); Yang et al. (2010); Rodríguez-Tembleque et al. (2013)], the material properties estimation [Buryachenko (2012); Buryachenko et al. (2012)], the shape optimization processes [Prochazka and Valek (2012)], the comparison between experimental and computational models [Selvadurai and Nikopour (2012)] and so on. For specific applications, a valid alternative could be glass fiber reinforced composites which have important properties but a mass density greater than carbon fibre reinforced composites [Samborsky et al. (2016); Sanjay et al. (2016); Shah et al. (2013)].

In recent years, natural fibre composites based on renewable resources can provide viable low-cost structural components and eco-friendly alternatives to conventional structural materials for automotive, aerospace and construction applications [Kim (2012)]. The growth in applications of natural fibre composites has increased the importance of understanding their properties such as creep resistance, stress relaxation and fatigue [Misra et al. (2011); Carrino and Durante (2011)]. Several natural fibres, such as hemp, flax, sisal, kenaf and jute, have been used in different industrial applications. Recently, natural fibres have obtained the interest of researchers, engineers and scientists as substitute reinforcements for fibre reinforced polymer composites. Due to their fairly good mechanical properties, low cost, high specific strength, environmentally-friendliness and bio-degradability, ease of fabrication and good structural rigidity, these materials can be used in an extensive range of applications [Alkbir et al. (2016)]. More recently, natural fibre composites have provided a solution for the manufacture of

fibre composite boats and surfboards with enhanced eco-profiles, even if they suffer from questionable environmental stability [Ansell (2014)]. The knowledge of the behaviour of natural fibres is of crucial importance for their use as a reinforcement for composites materials. Baley (2002) tested flax fibres under tensile loading and in repeated loading-unloading experiments. An important feature is the study of thermal decomposition of natural fibre composites as proposed by Fan and Naughton (2016). In this case, Dynamic Mechanical Analysis (DMA) could be a versatile technique that complements the information provided by the more traditional thermal analysis techniques such as differential scanning calorimetry, thermogravimetric analysis and thermo-mechanical analysis [Saba et. al (2016)]. In general, despite of significant research on the mechanical properties of fibre-reinforced polymer composites made of natural fibres, long-term performance of the natural fibre composites against moisture and other environmental conditions is not well-known and this feature must be necessary investigated [Hristozov et al. (2015); Summerscales and Grove (2014)]. An interesting review paper about natural fibres, their physical properties, fibre fabric types, fabrication methods, stacking sequence and failure criteria is that by Jauhari et al. (2015). The use of natural fibre composites leads to the so-called eco-design which is mainly carried out through Life Cycle Assessment tool by companies, in the post-production stage of parts, to provide useful information for the next production [Le Duigou and Baley (2014)]. There has been a rapid growth in research and innovation in the natural fibre composite area. Interest is warranted due to the advantages of these materials compared to others such as synthetic fibre composites. These advantages include low environmental impact, low cost and support for a wide range of applications [Pickering et al. (2016); Pickering and Le (2016)]. Compressive properties of three different natural fibre composites (flax, bamboo and coir fibre) have been measured in Van vuure et al. (2015) and Weclawski et al. (2014) in order to demonstrate their good specific mechanical properties.

The present paper proposes a comparative study between composite structures including different fiber reinforcements, in particular carbon fibres, glass fibers and linoleum fibers. A three-dimensional exact shell solution [Brischetto (2013); Brischetto (2014a); Brischetto (2015); Brischetto (2016a); Brischetto (2016b)] is used for the free vibration analysis of laminated symmetric and antisymmetric composite plates, cylinders, cylindrical and spherical shell panels. Simply supported boundary conditions are considered in order to obtain analytical solutions. The equilibrium shell equations in general orthogonal curvilinear coordinates are written and solved in layer-wise form using the exponential matrix method [Brischetto and Torre (2014); Brischetto et al. (2015); Brischetto et al. (2016b); Tornabene et al. (2015)]. The proposed model is a generalization of the previous 3D plate model in

orthogonal rectilinear coordinates by Messina (2009) and the previous 3D shell model in cylindrical coordinates by Soldatos and Ye (1995). The frequency comparisons are proposed for different geometries, materials, lamination sequences, vibration modes, half-wave numbers and thickness ratios. The main scope is to understand if the linoleum fibre composites are comparable, in terms of free vibration behavior, with carbon fibre and glass fibre composites. This study will need a further in-depth analysis also considering static, buckling and fatigue verifications.

Section 2 will propose a generic fibre classification where the main characteristics (advantages and disadvantages) are described. Section 3 will discuss the main elastic properties of the most common composites including natural and synthetic fibres. The 3D exact model will be shortly discussed in Section 4 and the main comparative results will be proposed in Section 5. The main conclusions will be shown in the last Section 6.

2 Fiber classification and main characteristics

Natural fibers are defined as materials obtained from renewable sources which can be easily recyclable or biodegradable [Ashby et al. (2013); Peek (2008)]. Terms usually employed in the case of natural fibers are bio-composites or eco-composites. Such composites can be obtained from different combinations [BAYDUR (2016); Bcomp (2016)]: - natural fibers in synthetic matrix; - natural fibers in renewable synthetic matrix; - synthetic fibers in biodegradable matrix; - synthetic fibres in renewable synthetic matrix; - natural fibers in natural matrix.

Natural fibres can have vegetable, animal or mineral origin. The first group includes fibers such as cotton, hemp and gaves. The second group includes silk and animal pelts. The third group includes materials such as asbestos which is very famous for its high level of danger [Performance Composites (2016)].

The bio-fibers have several advantages if compared with traditional fibers such as carbon and glass fibers [CW Composites World (2016)]: - low-cost; - abundant and easily procurable; - small problems from the respiratory and dermatologist point of view; - biodegradable, bio-compatible and recyclable using different matrices; - transformation processes at the end of life which use the combustion; - little abrasive; - smaller density than glass fibers; - similar density to carbon fibers; - increasing of acoustic and thermal insulation.

The three different composites compared in the present paper are those including carbon fibers,

glass fibers and linoleum fibers. Carbon fibers are usually employed to reinforce composites with polymeric matrices [Zoltek (2016)]. Their great diffusion is mainly due to their high strength combined with an elevated lightness. The main sectors where these fibers had a great diffusion are aerospace, automotive, rail transport, maritime transport and sport competitions. The main advantages are: - high elastic limit; - high fatigue resistance; - small weight; - low linear expansion coefficient; - they do not have in general corrosion phenomena; - they are not sensible to several chemical compounds; - good combustion resistance; - great integration in the structures which means reduction of the number of components. The main disadvantages are: - smaller compression resistance if compared with metals; - smaller impact resistance if compared with metals; - age with UAV rays, heat and humidity exposure; - high local damage if struck by lightning; - not easy to be repaired; - high costs; - not recyclable.

Glass fibers can be classified using their chemical composition and properties. E-glass is usually used for the electric insulation. S-glass has higher mechanical properties than the E-glass. R-glass has an excellent mechanical behavior and for this reason it is used in leading sectors such as aerospace and aviation. D-glass has small electric losses. AR-glass is usually used to reinforce the cement [Cristaldi (2012)]. C-glass is usually used for external coverings. The main sectors where these fibers had a great diffusion are aeronautics, automotive, nautical science, wind energy and sport competitions. The main advantages are: - low cost; - high speed production; - good resistance and rigidity; - thermal resistance; - good resistance to chemical factors; - low hygrometric sensitivity; - properties preservation in several conditions; - electric insulation. The main disadvantages are: - self-abrasion which reduces the resistance; - low fatigue resistance; - bigger mass density than carbon and natural fibers; - Young modulus smaller than other fibers.

Linoleum fibers are made, for 70%, of cellulose. Their main advantages are: - environmentally-friendly; - low production costs; - low weight; - good specific properties; - recyclable. The main disadvantages are: - variable fiber quality; - difficulties for the connections; - hygrometric sensitivity; - difficulties for the adhesion matrix-fibers. The main applications are in the sport competitions for the production of skies, snowboards, skateboards, bikes and aquatic equipments, in the transport for the production of structural panels (in particular in the automotive field [Lotus Car (2016)]), in the acoustic field for the production of musical instruments, in the design to obtain sustainable products, and in combination with carbon fibers to reduce the vibrations.

3 Elastic properties of composites including natural and synthetic fibers

Three different fibre reinforced composite materials will be compared in the present work in terms of free frequency values. These materials are a carbon fibre reinforced composite (see second column in Table 1), a glass fiber reinforced composite (see third column in Table 1) and a linoleum fiber reinforced composite (see fourth column in Table 1). Elastic properties and mass density are given for each proposed material. The carbon fibre composite properties have been obtained from the Composite Materials Handbook (2002), the glass fiber composite properties have been proposed in Samborsky et al. (2016) and the linoleum fiber composite properties have been described in Hosseini et al. (2015). These materials will be used with different lamination sequences and in different structures for a three-dimensional shell analysis, in terms of frequency, when a free vibration problem is solved. From Table 1, it is clear the supremacy of the carbon fibre composite with respect the other two composites. It has high elastic properties and small mass density, its specific properties (elastic properties divided with respect the mass density) are very high. The other two materials seem comparable between them, in fact the elastic properties of the glass fibre composite are slightly higher then those of the linoleum fibre composite but its density is about two times the density of the linoleum fibre composite (1900kg/m^3 vs. 1100kg/m^3). These features give similar specific properties for these two materials. This last consideration could mean that in a free vibration analysis, these two materials could have similar behaviors. In fact, the frequency values are proportional to $\sqrt{\frac{\mathrm{K}}{\mathrm{M}}}$ where K is the stiffness matrix which depends on the elastic properties and M is the inertial matrix which depends on the mass density. If the linoleum fibre composite will have a structural behavior similar to the glass fibre composite, this feature could be an advantage because of the low production costs and the low environmental impact of this natural fibre composite with respect to synthetic fibre composites.

4 Three-dimensional shell model

In the free vibration analysis proposed in Section 5, a three-dimensional exact shell model is used. This model has been developed in Brischetto (2013), Brischetto (2014a), Brischetto (2014b) and Brischetto (2014c). The equilibrium equations for shells are written in a general orthogonal curvilinear coordinate system, valid for plates and shells with constant radii of curvature, and they are solved in exact form

supposing simply supported structures and using the exponential matrix method. Similar models have been developed by Messina (2009) in rectilinear orthogonal coordinates for plates and by Soldatos and Ye (1995) for cylindrical coordinates.

The three differential equations of equilibrium written for the free vibration analysis of multilayered spherical shells made of N_L layers with constant radii of curvature R_α and R_β are:

$$H_\beta \frac{\partial \sigma^k_{\alpha\alpha}}{\partial \alpha} + H_\alpha \frac{\partial \sigma^k_{\alpha\beta}}{\partial \beta} + H_\alpha H_\beta \frac{\partial \sigma^k_{\alpha z}}{\partial z} + (\frac{2H_\beta}{R_\alpha} + \frac{H_\alpha}{R_\beta})\sigma^k_{\alpha z} = \rho^k H_\alpha H_\beta \ddot{u}^k \ , \tag{1}$$

$$H_\beta \frac{\partial \sigma^k_{\alpha\beta}}{\partial \alpha} + H_\alpha \frac{\partial \sigma^k_{\beta\beta}}{\partial \beta} + H_\alpha H_\beta \frac{\partial \sigma^k_{\beta z}}{\partial z} + (\frac{2H_\alpha}{R_\beta} + \frac{H_\beta}{R_\alpha})\sigma^k_{\beta z} = \rho^k H_\alpha H_\beta \ddot{v}^k \ , \tag{2}$$

$$H_\beta \frac{\partial \sigma^k_{\alpha z}}{\partial \alpha} + H_\alpha \frac{\partial \sigma^k_{\beta z}}{\partial \beta} + H_\alpha H_\beta \frac{\partial \sigma^k_{zz}}{\partial z} - \frac{H_\beta}{R_\alpha}\sigma^k_{\alpha\alpha} - \frac{H_\alpha}{R_\beta}\sigma^k_{\beta\beta} + (\frac{H_\beta}{R_\alpha} + \frac{H_\alpha}{R_\beta})\sigma^k_{zz} = \rho^k H_\alpha H_\beta \ddot{w}^k \ , \tag{3}$$

where ρ^k is the mass density, $(\sigma^k_{\alpha\alpha}, \sigma^k_{\beta\beta}, \sigma^k_{zz}, \sigma^k_{\beta z}, \sigma^k_{\alpha z}, \sigma^k_{\alpha\beta})$ are the six stress components and $\ddot{u}^k$, $\ddot{v}^k$ and $\ddot{w}^k$ indicate the second temporal derivative of the three displacement components. Each quantity depends on the k layer. R_α and R_β are referred to the mid-surface Ω_0 of the whole multilayered shell. H_α and H_β continuously vary through the thickness of the multilayered shell and they depend on the thickness coordinate z. The middle surface Ω_0 of the shell is the locus of points which lie midway between these surfaces. Geometry and the curvilinear orthogonal reference system (α, β, z) are shown in Figure 1. Displacement components are u, v, and w in α, β and z directions, respectively. The parametric coefficients for shells with constant radii of curvature are:

$$H_\alpha = (1 + \frac{z}{R_\alpha}) \ , \quad H_\beta = (1 + \frac{z}{R_\beta}) \ , \quad H_z = 1 \ , \tag{4}$$

H_α and H_β depend on z coordinate.

For simply supported shells and plates, the three displacement components have the following harmonic form:

$$u^j(\alpha, \beta, z, t) = U^j(z) e^{i\omega t} cos(\bar{\alpha}\alpha) sin(\bar{\beta}\beta) \ , \tag{5}$$

$$v^j(\alpha, \beta, z, t) = V^j(z) e^{i\omega t} sin(\bar{\alpha}\alpha) cos(\bar{\beta}\beta) \ , \tag{6}$$

$$w^j(\alpha, \beta, z, t) = W^j(z) e^{i\omega t} sin(\bar{\alpha}\alpha) sin(\bar{\beta}\beta) \ , \tag{7}$$

where U^j(z), V^j(z) and W^j(z) are the displacement amplitudes in α, β and z directions, respectively. i

is the coefficient of the imaginary unit. $\omega = 2\pi$f is the circular frequency where f is the frequency value, t is the time. In coefficients $\bar{\alpha} = \frac{m\pi}{a}$ and $\bar{\beta} = \frac{n\pi}{b}$, m and n are the half-wave numbers and a and b are the shell dimensions in α and β directions, respectively (calculated in the mid-surface Ω_0).

Substituting Eqs.(5)-(7) and constitutive and geometrical equations (given in details in Brischetto (2013)), the following final system is obtained:

$$\boldsymbol{D}^j \frac{\partial \boldsymbol{U}^j}{\partial z} = \boldsymbol{A}^j \boldsymbol{U}^j \ , \tag{8}$$

where $\frac{\partial \boldsymbol{U}^j}{\partial z} = \boldsymbol{U}^{j\prime}$ and $\boldsymbol{U}^j = [U^j \ V^j \ W^j \ U^{j\prime} \ V^{j\prime} \ W^{j\prime}]$. Eq.(8) can be rewritten as:

$$\boldsymbol{D}^j \boldsymbol{U}^{j\prime} = \boldsymbol{A}^j \boldsymbol{U}^j \ , \tag{9}$$

$$\boldsymbol{U}^{j\prime} = \boldsymbol{D}^{j\,-1} \boldsymbol{A}^j \ \boldsymbol{U}^j \ , \tag{10}$$

$$\boldsymbol{U}^{j\prime} = \boldsymbol{A}^{j*} \ \boldsymbol{U}^j \ , \tag{11}$$

with $\boldsymbol{A}^{j*} = \boldsymbol{D}^{j\,-1} \boldsymbol{A}^j$.

The solution of Eq.(11), as proposed in Brischetto (2013), is:

$$\boldsymbol{U}^j(z^j) = exp(\boldsymbol{A}^{j*} z^j) \boldsymbol{U}^j(0) \quad \text{with} \quad z^j \ \epsilon \ [0, h^j] \ , \tag{12}$$

where z^j is the thickness coordinate of each j layer from 0 at the bottom to h^j at the top. The exponential matrix is calculated with z^j=h^j for each j layer as:

$$\boldsymbol{A}^{j**} = exp(\boldsymbol{A}^{j*} h^j) = \boldsymbol{I} + \boldsymbol{A}^{j*} h^j + \frac{\boldsymbol{A}^{j*2}}{2!} {h^j}^2 + \frac{\boldsymbol{A}^{j*3}}{3!} {h^j}^3 + \ldots + \frac{\boldsymbol{A}^{j*N}}{N!} {h^j}^N \ , \tag{13}$$

where $\boldsymbol{I}$ is the 6×6 identity matrix. This expansion has a fast convergence and it is not time consuming from the computational point of view.

Considering j=M mathematical layers to approximate the shell curvature, M-1 transfer matrices must be calculated using for each interface the interlaminar continuity conditions of displacements and transverse shear/normal stresses. Moreover, the structures must be considered as simply supported and free stresses at the top and at the bottom. All these conditions allow the following final system to be obtained:

$$\boldsymbol{E} \, \boldsymbol{U}^1(0) \ = \ \boldsymbol{0} \ , \tag{14}$$

where matrix $\boldsymbol{E}$ has always (6×6) dimension, independently from the number of layers M, even if the method uses a layer-wise approach. $\boldsymbol{U}^1(0)$ means $\boldsymbol{U}$ calculated at the bottom of the whole multilayered shell (first layer 1 with z^1=0). Further details about this procedure, and all the steps missed in this paper can be found in Brischetto (2013), Brischetto (2014a), Brischetto (2014b) and Brischetto (2014c) where the extensions of this 3D exact method have been made for the first time. The proposed has also been validated in these past works, and it can be now used with confidence for the results proposed in Section 5.

The free vibration analysis means to find the non-trivial solution of $\boldsymbol{U}^1(0)$ in Eq.(14) imposing the determinant of matrix $\boldsymbol{E}$ equals zero:

$$det[\boldsymbol{E}] = 0\,, \tag{15}$$

Eq.(15) allows to calculate the roots of an higher order polynomial in $\lambda = \omega^2$. For each pair of half-wave numbers (m,n), a certain number of circular frequencies $\omega = 2\pi$f (from I to ∞) are obtained. This number depends on the order N chosen for each exponential matrix $\boldsymbol{A}^{j**}$ and the number M of mathematical layers. From the validations proposed in Brischetto (2016a) and Brischetto (2016b), N=3 and M=100 or M=102 are sufficient to always obtain the correct results for each geometry, lamination sequence, number of layers, material and thickness ratio

5 Results

The investigated geometries are plates, cylinders, cylindrical shell panels and spherical shell panels (see Figure 1). The geometrical data of these structures are detailed in Table 2 where the in-plane dimensions a and b and the radii of curvature R_α and R_β are given for each structure. As indicated in Figure 1, each geometry can be three-layered symmetric $0°/90°/0°$ and four-layered antisymmetric $0°/90°/0°/90°$. For each geometry and for each lamination sequence, the three materials described in Table 1 have been employed. Table 1 contains the elastic properties and the mass density for a carbon fibre reinforced composite, a glass fibre reinforced composite and a linoleum fibre reinforced composite. These three materials will be compared in this section, using the three-dimensional exact shell model proposed in Section 4, in terms of free frequencies for several geometries, thickness ratios, lamination sequences, vibration modes and imposed half-wave numbers. The considered thickness ratios a/h for plates are 100, 50, 20 and 10. The considered thickness ratios R_α/h for shells are 1000, 100, 10 and 5.

Tables 3 and 4 show the free frequency f in Hz for symmetrical and antisymmetrical composite

plates. The first three modes (from I to III) for half-wave numbers m=n equal 1, 2 and 3 are calculated for different thickness ratios a/h and for the three proposed composite materials. It is clear how the frequencies for glass and linoleum fibre reinforced composites are close for each thickness ratio, lamination sequence, vibration mode and half-wave numbers. The frequency values for carbon fibre composites are much more different. All these considerations are confirmed by Figure 2 where thick and thin symmetric and antisymmetric plates are investigated. Black curves are for the carbon fibre composite material, red curves are for the glass fibre composite material and the blue curves are for the linoleum fibre composite material. Red and blue curves are very close for each thickness ratio and lamination sequence when half-wave number n varies from 1 to 4 and half-wave number m varies from 1 to 7. For this large range of half-wave numbers, the carbon fibre composite behavior is completely different from the behavior of the other two composites. Glass and linoleum fibre reinforced composites have a similar behavior in terms of free frequency values.

The same investigation is repeated in Tables 5 and 6 for symmetrical and antisymmetrical cylinders, respectively. The first three modes (I, II and III) in Hz are proposed for longitudinal half-wave number m=1 and circumferential half-wave numbers n equal 2, 4 and 6 (only even values because the cylinder is closed in β direction). The three proposed composites are compared for different thickness ratios R_α/h. The behavior of the glass fibre composite and the linoleum fibre composite is very similar. The carbon fibre composite has the best performances in relation to the free vibration analysis. These considerations are confirmed by Figure 3. Thin shells are in the left part of the figure, thick shells are in right part of the figure. The two top images are for the symmetric configurations, the two bottom images are for the antisymmetric configurations. The behavior of glass and linoleum fibre composites is very similar for a large variety of imposed half-wave numbers m and n.

The cylindrical shell panel including the three proposed materials is investigated in Tables 7 and 8 for symmetrical and antisymmetrical configurations, respectively. Conclusions are similar to those already obtained for the cylinder case. The investigated half-wave numbers are m=n equal 1, 2 and 3. For each (m,n) couple, the first three modes are proposed in the case of thick and thin shells. The performances of the linoleum fibre composite are very lower than the carbon fibre composite, but they are comparable with those obtained for the glass fibre composite. These considerations are confirmed by the graphical results proposed in Figure 4 where a large variety of half-wave numbers m and n is investigated for the first mode in Hz.

All the considerations proposed above are also confirmed for the last proposed geometry which is

a spherical shell panel with the same radii of curvature R_α=R_β in the two in-plane directions. Tables 9 and 10 show results for symmetrical and antisymmetrical laminations, respectively. The first three modes (I, II and III) in Hz are proposed for the three different materials when m=n=1, m=n=2 and m=n=3. Both thick and thin shells are investigated. The linoleum fibre reinforced composite has a similar behavior, in terms of free frequencies, to the glass fibre reinforced composite. On the contrary, the performances of the carbon fibre composite are clearly better than the other two investigated composites. All these considerations are confirmed by the graphical results proposed in Figure 5 where the red and blue curves (for glass and linoleum fibre composites, respectively) are always very close between them for each lamination sequence (antisymmetric or symmetric), thickness ratio (thick and thin spherical shells) and half-wave numbers m and n.

Figures 2-5 confirm that the first frequency is monotonic increasing, in the case of plate geometry, when both half-wave numbers m and/or n increase. This behavior is not confirmed for the shell geometries, where the minimum frequency value is obtained for half-wave numbers m and n different from one. This behavior is due to the fact that in shell geometries, the three displacement components are completely coupled due to the presence of the curvature terms.

6 Conclusions

The present work proposed a comparative study for three different composite materials: a carbon fibre reinforced material, a glass fibre reinforced material and a linoleum fibre reinforced material. This last composite includes natural fibres which have a low-cost production and a low-environmental impact. These three composite materials have been included in plate, cylinder, cylindrical shell and spherical shell geometries with different thickness ratios and symmetrical and antisymmetrical laminations. The comparison is conducted using a three-dimensional exact shell model which allows a free vibration analysis of simply supported structures. The proposed investigation confirms the well-known superiority of the carbon fiber reinforced composites. Linoleum fiber reinforced composites and glass fiber reinforced composites have a similar behavior in terms of free frequencies. This similarity is confirmed for all the proposed geometries, thickness ratios, lamination sequences, vibration modes and a large spectrum of half-wave numbers. This first partial conclusion, based on a free vibration analysis, needs further confirmations via static, buckling and fatigue analyses. Only after these further investigations, it will be possible to confirm the convenient use of linoleum fiber composites in several engineering applications.

Bibliography

Alkbir, M.F.M.; Sapuan, S.M.; Nuraini, A.A.; Ishak, M.R. (2016): Fibre properties and crashworthiness parameters of natural fibre-reinforced composite structure: a literature review. *Composite Structures*, vol. 148, pp. 59-73.

Allix, O.; Kerfriden, P.; Gosselet, P. (2010): A relocalization technique for the multiscale computation of delamination in composite structures. *CMES: Computer Modeling in Engineering & Sciences*, vol. 55, pp. 271-292.

Ansell, M.P. (2014): Natural fibre composites in a marine environment. *Natural Fibre Composites. Materials, Processes and Applications*, Edited by: A. Hodzic and R. Shanks, pp. 365-374.

Ashby, M.; Shercliff, H.; Cebon, D. (2013): Materials: Engineering, Science, Processing and Design. Butterworth-Heinemann, Oxford.

Baley, C. (2002): Analysis of the flax fibres tensile behaviour and analysis of the tensile stiffness increase. *Composites Part A: Applied Science and Manufacturing*, vol. 33, pp. 939-948.

Baltacoglu, A.; Civalek, O (2010): Geometrically nonlinear analysis of anisotropic composite plates resting on nonlinear elastic foundations. *CMES: Computer Modeling in Engineering & Sciences*, vol. 68, pp. 1-24.

BAYDUR Trial Product PU 60BD33, available on http://www.gammapoliuretani.com/pdf, accessed on 26th May 2016.

Bcomp natural fibre composites, available on http://www.bcomp.ch/, accessed on 26th May 2016.

Brischetto, S. (2013): Exact elasticity solution for natural frequencies of functionally graded simply-supported structures. *CMES: Computer Modeling in Engineering & Sciences*, vol. 95, pp. 391-430.

Brischetto, S. (2014a): A continuum elastic three-dimensional model for natural frequencies of single-walled carbon nanotubes. *Composites: Part B*, vol. 61, pp. 222-228.

Brischetto, S. (2014b): Three-dimensional exact free vibration analysis of spherical, cylindrical and flat one-layered panels. *Shock and Vibration*, vol. 2014, pp. 1-29.

Brischetto, S. (2014c): An exact 3D solution for free vibrations of multilayered cross-ply composite and sandwich plates and shells. *International Journal of Applied Mechanics*, vol. 6, pp. 1-42.

Brischetto, S. (2014d): Innovative multilayered structures for a new generation of aircraft and spacecraft. *Journal of Aeronautics & Aerospace Engineering*, vol. 4, pp. 1-2.

Brischetto, S. (2015): A continuum shell model including van derWaals interaction for free vibrations

of double-walled carbon nanotubes. *CMES: Computer Modeling in Engineering & Sciences*, vol. 104, pp. 305-327.

Brischetto, S. (2016a): Exact and approximate shell geometry in the free vibration analysis of one-layered and multilayered structures. *International Journal of Mechanical Sciences*, vol. 113, pp. 81-93.

Brischetto, S. (2016b): Convergence analysis of the exponential matrix method for the solution of 3D equilibrium equations for free vibration analysis of plates and shells. *Composites: Part B*, vol. 98, pp. 453-471.

Brischetto, S.; Torre, R. (2014): Exact 3D solutions and finite element 2D models for free vibration analysis of plates and cylinders. *Curved and Layered Structures*, vol. 1, pp. 59-92.

Brischetto, S.; Tornabene, F.; Fantuzzi, N.; Bacciocchi, M. (2015): Refined 2D and exact 3D shell models for the free vibration analysis of single- and double-walled carbon nanotubes. *Technologies*, vol. 3, pp. 259-284.

Brischetto, S.; Ciano, A.; Ferro, C.G. (2016a): A multipurpose modular drone with adjustable arms produced via the FDM additive manufacturing process. *Curved and Layered Structures*, vol. 3, pp. 202-213.

Brischetto, S.; Tornabene, F.; Fantuzzi, N.; Viola, E. (2016b): 3D exact and 2D generalized differential quadrature models for free vibration analysis of functionally graded plates and cylinders. *Meccanica*, in press.

Buryachenko, V.A. (2012): Modeling of random bimodal structures of composites (application to solid propellants): II. Estimation of effective elastic moduli. *CMES: Computer Modeling in Engineering & Sciences*, vol. 85, pp. 417-446.

Buryachenko, V.A.; Jackson, T.L.; Amadio, G. (2012): Modeling of random bimodal structures of composites (application to solid propellants): I. Simulation of random packs. *CMES: Computer Modeling in Engineering & Sciences*, vol. 85, pp. 379-416.

Carrino, L.; Durante, M. (2011): Realizzazione e Caratterizzazione di Laminati in Composito Polimerico Termoplastico Rinforzato con Fibre Naturali. Produzione di Laminati con Fibre Naturali e loro Caratterizzazione. Research report. Universitá degli Studi di Napoli "Federico II".

Cristaldi, G. (2012): Sviluppo di Materiali Compositi Rinforzati con Fibre Naturali per l'Ingegenria Civile. Ph.D. Thesis. Universitá degli Studi di Catania.

CW Composites World, available on http://www.compositesworld.com/articles/eco-elise-concept-lean-speedy-and-green, accessed on 26th May 2016.

Department of Defense Handbook (2002): Composite Materials Handbook Volume 3. Polymer Matrix Composites Materials. Usage, Design, and Analysis.

Fan, M.; Naughton, A. (2016): Mechanisms of thermal decomposition of natural fibre composites. *Composites Part B: Engineering*, vol. 88, pp. 1-10.

Ferro, C.G.; Brischetto, S.; Torre, R.; Maggiore, P. (2016): Characterization of ABS specimens produced via the 3D printing technology for drone structural components. *Curved and Layered Structures*, vol. 3, pp. 172-188.

Hosseini, N.; Javid, S.; Amiri, A.; Ulven, C.; Webster, D.C.; Karami, G. (2015): Micromechanical viscoelastic analysis of flax fiber reinforced bio-based polyurethane composites. *Journal of Renewable Materials*, vol. 3, pp. 205-215.

Hristozov, D.; Wroblewski, L.; Sadeghian, P. (2015): Long-term tensile properties of natural fibre-reinforced polymer composites: comparison of flax and glass fibres. *Composites Part B: Engineering*, vol. 95, pp. 82-95.

Hwu, C.; Yu, M. (2010): A comprehensive finite element model for tapered composite wing structures. *CMES: Computer Modeling in Engineering & Sciences*, vol. 67, pp. 151-174.

Jauhari, M.; Mishra, R.; Thakur, H. (2015): Natural fibre reinforced composite laminates: a review. *Materials Today: Proceedings*, vol. 2, pp. 2868-2877.

Kim, Y.K. (2012): Natural fibre composites (NFCs) for construction and automotive industries. *Handbook of Natural Fibres. Processing and Applications*, Edited by: R. Kozlowski , pp. 254-279.

Le Duigou, A.; Baley, C. (2014): Coupled micromechanical analysis and life cycle assessment as an integrated tool for natural fibre composites development. *Journal of Cleaner Production*, vol. 83, pp. 61-69.

Lotus Car, available on http://www.lotuscars.com/, accessed on 26th May 2016.

Messina, A. (2009): Three Dimensional Free Vibration Analysis of Cross-Ply Laminated Plates through 2D and Exact Models. *3rd International Conference on Integrity, Reliability and Failure*, Porto (Portugal).

Misra, M.; Ahankari, S.S.; Mohanty, A.K.; Nga, A.D. (2011): Creep and fatigue of natural fibre composites. *Interface Engineering of Natural Fibre Composites for Maximum Performance*, Edited by: N.E. Zafeiropoulos, pp. 289-340.

Peek, N. (2008): Rapid Prototyping of Green Composites. Mester Degree Thesis. University of Amsterdam.

Performance Composites, available on http://www.performance-composites.org/, accessed on 26th May 2016.

Pickering, K.L.; Aruan Efendy, M.G.; Le, T.M. (2016): A review of recent developments in natural fibre composites and their mechanical performance. *Composites Part A: Applied Science and Manufacturing*, vol. 83, pp. 98-112.

Pickering, K.L.; Le, T.M. (2012): High performance aligned short natural fibre - Epoxy composites. *Composites Part B: Engineering*, vol. 85, pp. 123-129.

Prochazka, P.P.; Valek, M.J. (2012): Optimal shape of fibers in transmission problem. *CMES: Computer Modeling in Engineering & Sciences*, vol. 87, pp. 207-224.

Rodríguez-Tembleque, L.; Sáez, A.; Buroni, F.C. (2013): Numerical study of polymer composites in contact. *CMES: Computer Modeling in Engineering & Sciences*, vol. 96, pp. 131-158.

Rodríguez-Tembleque, L.; Aliabadi, M.H. (2014): Friction and wear modelling in fiber-reinforced composites. *CMES: Computer Modeling in Engineering & Sciences*, vol. 102, pp. 183-210.

Saba, N.; Jawaid, M.; Alothman, O.Y.; Paridah, M.T. (2016): A review on dynamic mechanical properties of natural fibre reinforced polymer composites. *Construction and Building Materials*, vol. 106, pp. 149-159.

Samborsky, D.D.; Mandell, J.F.; Agastra, P.: 3D Static Elastic Constants and Strength Properties of a Glass/Epoxy Unidirectional Laminate. Composite Technologies Research Group - Montana State University. Available on http://www.coe.montana.edu/composites/, accessed on 26th May 2016.

Sanjay, M.R.; Arpitha, G.R.; Yogesha, B. (2016): Study on mechanical properties of natural-glass fibre reinforced polymer hybrid composites: a review. *Materials Today: Proceedings*, vol. 2, pp. 2959-2967.

Selvadurai, A.P.S.; Nikopour, H. (2012): Uniform loading of a cracked layered composite plate: experiments and computational modelling. *CMES: Computer Modeling in Engineering & Sciences*, vol. 85, pp. 279-298.

Shah, D.U.; Schubel, P.J.; Clifford, M.J. (2013): Can flax replace E-glass in structural composites? A small wind turbine blade case study. *Composites: Part B*, vol. 52, pp. 172-181.

Soldatos, K.P.; Ye, J. (1995): Axisymmetric static and dynamic analysis of laminated hollow cylinders composed of monoclinic elastic layers. *Journal of Sound and Vibration*, vol. 184, pp. 245-259.

Summerscales, J.; Grove, S. (2014): Manufacturing methods for natural fibre composites. *Natural Fibre Composites. Materials, Processes and Applications*, Edited by: A. Hodzic and R. Shanks, pp.

176-215.

Távara, L.; Mantic, V.; Graciani, E.; Cañas, J.; París, F. (2010): Analysis of a crack in a thin adhesive layer between orthotropic materials: an application to composite interlaminar fracture toughness test. *CMES: Computer Modeling in Engineering & Sciences*, vol. 58, pp. 247-270.

Tornabene, F.; Brischetto, S.; Fantuzzi, N.; Viola, E. (2015): Numerical and exact models for free vibration analysis of cylindrical and spherical shell panels. *Composites: Part B*, vol. 81, pp. 231-250.

Valisetty, R.; Rajendran, A.; Grove, D. (2010): Mesh effects in predictions of progressive damage in 3D woven composites. *CMES: Computer Modeling in Engineering & Sciences*, vol. 60, pp. 41-72.

Van Vuure, A.W.; Baets, J.; Wouters, K.; Hendrickx, K. (2015): Compressive properties of natural fibre composites. *Materials Letters*, vol. 149, pp. 138-140.

Weclawski, B.T.; Fan, M.; Hui, D. (2014): Compressive behaviour of natural fibre composite. *Composites Part B: Engineering*, vol. 67, pp. 183-191.

Yang, B.; Ouyang, J.; Jiang, T.; Liu, C. (2010): Modeling and simulation of fiber reinforced polymer mold filling process by level set method. *CMES: Computer Modeling in Engineering & Sciences*, vol. 63, pp. 191-222.

Zoltek Commercial Carbon Fiber, available on http://zoltek.com/carbonfiber/, accessed on 26th May 2016.

Properties	Carbon fiber composite	Glass fiber composite	Linoleum fiber composite
E_1[GPa]	113.6	44.60	28.75
E_2[GPa]	9.650	17.00	4.310
E_3[GPa]	9.650	16.70	4.290
ν_{12}[-]	0.334	0.262	0.370
ν_{13}[-]	0.328	0.264	0.360
ν_{23}[-]	0.490	0.350	0.480
G_{12}[GPa]	6.000	3.490	2.210
G_{13}[GPa]	6.000	3.770	2.230
G_{23}[GPa]	3.100	3.460	1.490
ρ[kg/m^3]	1265	1900	1100

Table 1: Elastic and mass properties of the three considered composites.

Properties	Plate	Cylinder	Cylindrical shell	Spherical shell
a[m]	1.0	$2\pi R_\alpha$	$\pi/3R_\alpha$	$\pi/3R_\alpha$
b[m]	1.0	20	20	$\pi/3R_\alpha$
R_α[m]	∞	10	10	10
R_β[m]	∞	∞	∞	10

Table 2: Geometrical data of the four considered structures.

Mode	I	II	III
		a/h=100	
		m=1, n=1	
Carbon fiber (f[Hz])	50.114	3093.3	4170.0
Glass fiber (f[Hz])	30.549	1841.5	2418.7
Linoleum fiber (f[Hz])	29.249	1746.8	2371.3
		m=2, n=2	
Carbon fiber (f[Hz])	199.63	6184.3	8338.1
Glass fiber (f[Hz])	121.94	3682.7	4837.1
Linoleum fiber (f[Hz])	116.70	3493.1	4742.0
		m=3, n=3	
Carbon fiber (f[Hz])	446.13	9271.1	12502
Glass fiber (f[Hz])	273.39	5523.7	7254.8
Linoleum fiber (f[Hz])	261.45	5238.3	7111.2
		a/h=50	
		m=1, n=1	
Carbon fiber (f[Hz])	99.815	3092.2	4169.0
Glass fiber (f[Hz])	60.969	1841.4	2418.5
Linoleum fiber (f[Hz])	58.349	1746.5	2371.0
		m=2, n=2	
Carbon fiber (f[Hz])	392.88	6175.6	8330.2
Glass fiber (f[Hz])	241.83	3682.0	4835.8
Linoleum fiber (f[Hz])	231.04	3491.0	4739.1
		m=3, n=3	
Carbon fiber (f[Hz])	861.75	9241.7	12475
Glass fiber (f[Hz])	536.73	5521.3	7250.4
Linoleum fiber (f[Hz])	511.39	5231.3	7101.2
		a/h=20	
		m=1, n=1	
Carbon fiber (f[Hz])	242.70	3084.5	4162.1
Glass fiber (f[Hz])	150.21	1840.7	2417.4
Linoleum fiber (f[Hz])	143.33	1744.7	2368.4
		m=2, n=2	
Carbon fiber (f[Hz])	890.81	6115.1	8273.3
Glass fiber (f[Hz])	572.50	3677.1	4826.5
Linoleum fiber (f[Hz])	541.41	3476.4	4717.9
		m=3, n=3	
Carbon fiber (f[Hz])	1791.9	9040.0	12272
Glass fiber (f[Hz])	1201.4	5504.9	7218.1
Linoleum fiber (f[Hz])	1124.0	5182.6	7026.8
		a/h=10	
		m=1, n=1	
Carbon fiber (f[Hz])	445.41	3057.5	4136.6
Glass fiber (f[Hz])	286.25	1838.6	2413.2
Linoleum fiber (f[Hz])	270.70	1738.2	2359.0
		m=2, n=2	
Carbon fiber (f[Hz])	1415.9	5906.8	8038.0
Glass fiber (f[Hz])	984.40	3660.0	4790.8
Linoleum fiber (f[Hz])	911.82	3425.7	4633.5
		m=3, n=3	
Carbon fiber (f[Hz])	2559.9	8392.4	10922
Glass fiber (f[Hz])	1864.1	5449.5	7082.7
Linoleum fiber (f[Hz])	1703.5	5018.6	6684.7

Table 3: Symmetric $0°/90°/0°$ composite plate. First three frequencies in Hz for several thickness ratios and imposed half-wave numbers.

Mode	I	II	III
		a/h=100	
		m=1, n=1	
Carbon fiber (f[Hz])	47.214	3413.2	3912.4
Glass fiber (f[Hz])	30.055	1886.7	2383.6
Linoleum fiber (f[Hz])	28.007	1861.5	2282.4
		m=2, n=2	
Carbon fiber (f[Hz])	188.28	6824.2	7822.1
Glass fiber (f[Hz])	119.98	3773.2	4766.8
Linoleum fiber (f[Hz])	111.79	3722.5	4564.0
		m=3, n=3	
Carbon fiber (f[Hz])	421.49	10231	11727
Glass fiber (f[Hz])	269.08	5659.3	7149.3
Linoleum fiber (f[Hz])	250.65	5582.3	6843.9
		a/h=50	
		m=1, n=1	
Carbon fiber (f[Hz])	94.139	3412.1	3911.1
Glass fiber (f[Hz])	59.991	1886.6	2383.4
Linoleum fiber (f[Hz])	55.895	1861.2	2282.0
		m=2, n=2	
Carbon fiber (f[Hz])	372.06	6815.6	7811.7
Glass fiber (f[Hz])	238.10	3772.4	4765.4
Linoleum fiber (f[Hz])	221.73	3720.3	4560.6
		m=3, n=3	
Carbon fiber (f[Hz])	821.10	10202	11691
Glass fiber (f[Hz])	528.97	5656.7	7144.5
Linoleum fiber (f[Hz])	492.19	5575.1	6832.2
		a/h=20	
		m=1, n=1	
Carbon fiber (f[Hz])	230.50	3404.6	3901.9
Glass fiber (f[Hz])	147.96	1885.9	2382.1
Linoleum fiber (f[Hz])	137.73	1859.3	2279.0
		m=2, n=2	
Carbon fiber (f[Hz])	862.15	6756.6	7736.7
Glass fiber (f[Hz])	565.75	3767.2	4755.1
Linoleum fiber (f[Hz])	525.18	3705.6	4536.0
		m=3, n=3	
Carbon fiber (f[Hz])	1767.6	10008	11427
Glass fiber (f[Hz])	1191.9	5639.5	7108.7
Linoleum fiber (f[Hz])	1102.5	5526.7	6746.1
		a/h=10	
		m=1, n=1	
Carbon fiber (f[Hz])	431.07	3378.3	3868.3
Glass fiber (f[Hz])	282.87	1883.6	2377.6
Linoleum fiber (f[Hz])	262.59	1852.8	2268.0
		m=2, n=2	
Carbon fiber (f[Hz])	1415.9	6560.5	7441.5
Glass fiber (f[Hz])	980.15	3749.8	4715.1
Linoleum fiber (f[Hz])	903.27	3656.4	4439.6
		m=3, n=3	
Carbon fiber (f[Hz])	2587.8	9410.8	10386
Glass fiber (f[Hz])	1864.9	5586.7	6952.2
Linoleum fiber (f[Hz])	1708.5	5376.3	6385.0

Table 4: Antisymmetric $0°/90°/0°/90°$ composite plate. First three frequencies in Hz for several thickness ratios and imposed half-wave numbers.

Mode	I	II	III
		R_α/h=1000	
		m=2, n=1	
Carbon fiber (f[Hz])	36.697	150.41	184.97
Glass fiber (f[Hz])	22.817	88.659	108.51
Linoleum fiber (f[Hz])	23.560	84.459	104.83
		m=4, n=1	
Carbon fiber (f[Hz])	21.832	162.55	287.70
Glass fiber (f[Hz])	13.656	99.794	161.07
Linoleum fiber (f[Hz])	13.835	94.059	160.31
		m=6, n=1	
Carbon fiber (f[Hz])	14.053	180.09	403.54
Glass fiber (f[Hz])	8.8111	111.21	224.06
Linoleum fiber (f[Hz])	8.7364	106.79	223.65
		R_α/h=100	
		m=2, n=1	
Carbon fiber (f[Hz])	36.698	150.40	184.96
Glass fiber (f[Hz])	22.818	88.659	108.51
Linoleum fiber (f[Hz])	23.561	84.457	104.83
		m=4, n=1	
Carbon fiber (f[Hz])	21.870	162.54	287.68
Glass fiber (f[Hz])	13.678	99.794	161.07
Linoleum fiber (f[Hz])	13.854	94.058	160.30
		m=6, n=1	
Carbon fiber (f[Hz])	14.450	180.09	403.50
Glass fiber (f[Hz])	8.9990	111.21	224.05
Linoleum fiber (f[Hz])	8.9339	106.79	223.64
		R_α/h=10	
		m=2, n=1	
Carbon fiber (f[Hz])	36.796	149.97	184.49
Glass fiber (f[Hz])	22.975	88.595	108.38
Linoleum fiber (f[Hz])	23.636	84.353	104.64
		m=4, n=1	
Carbon fiber (f[Hz])	25.019	162.17	285.95
Glass fiber (f[Hz])	15.593	99.775	160.55
Linoleum fiber (f[Hz])	15.582	93.988	159.57
		m=6, n=1	
Carbon fiber (f[Hz])	33.367	179.77	399.20
Glass fiber (f[Hz])	19.519	111.22	222.98
Linoleum fiber (f[Hz])	19.582	106.75	221.94
		R_α/h=5	
		m=2, n=1	
Carbon fiber (f[Hz])	37.079	148.68	182.79
Glass fiber (f[Hz])	23.417	88.398	107.94
Linoleum fiber (f[Hz])	23.854	84.038	103.96
		m=4, n=1	
Carbon fiber (f[Hz])	30.715	160.99	279.78
Glass fiber (f[Hz])	19.644	99.714	158.78
Linoleum fiber (f[Hz])	19.147	93.765	157.07
		m=6, n=1	
Carbon fiber (f[Hz])	50.249	178.74	383.51
Glass fiber (f[Hz])	31.783	111.22	219.24
Linoleum fiber (f[Hz])	31.134	106.60	215.94

Table 5: Symmetric $0°/90°/0°$ composite cylinder. First three frequencies in Hz for several thickness ratios and imposed half-wave numbers.

Mode	I	II	III
		R_α/h=1000	
		m=2, n=1	
Carbon fiber (f[Hz])	36.737	158.96	182.22
Glass fiber (f[Hz])	22.802	88.620	109.90
Linoleum fiber (f[Hz])	23.571	87.308	104.63
		m=4, n=1	
Carbon fiber (f[Hz])	22.330	185.86	256.42
Glass fiber (f[Hz])	13.809	105.77	152.04
Linoleum fiber (f[Hz])	14.174	104.24	145.75
		m=6, n=1	
Carbon fiber (f[Hz])	14.730	201.91	357.90
Glass fiber (f[Hz])	9.0282	117.20	209.96
Linoleum fiber (f[Hz])	9.1771	116.44	201.59
		R_α/h=100	
		m=2, n=1	
Carbon fiber (f[Hz])	36.778	158.87	182.36
Glass fiber (f[Hz])	22.815	88.586	109.94
Linoleum fiber (f[Hz])	23.594	87.258	104.71
		m=4, n=1	
Carbon fiber (f[Hz])	22.400	185.87	256.31
Glass fiber (f[Hz])	13.845	105.77	152.00
Linoleum fiber (f[Hz])	14.215	104.23	145.71
		m=6, n=1	
Carbon fiber (f[Hz])	14.994	201.94	357.61
Glass fiber (f[Hz])	9.1943	117.20	209.87
Linoleum fiber (f[Hz])	9.3305	116.44	201.47
		R_α/h=10	
		m=2, n=1	
Carbon fiber (f[Hz])	37.543	157.51	183.36
Glass fiber (f[Hz])	23.179	88.150	110.29
Linoleum fiber (f[Hz])	24.012	86.622	105.30
		m=4, n=1	
Carbon fiber (f[Hz])	25.504	185.53	253.16
Glass fiber (f[Hz])	15.794	105.64	151.18
Linoleum fiber (f[Hz])	15.985	103.99	144.63
		m=6, n=1	
Carbon fiber (f[Hz])	28.709	201.84	349.24
Glass fiber (f[Hz])	18.097	117.18	207.87
Linoleum fiber (f[Hz])	17.340	116.35	198.43
		R_α/h=5	
		m=2, n=1	
Carbon fiber (f[Hz])	38.922	154.83	183.43
Glass fiber (f[Hz])	23.985	87.445	110.47
Linoleum fiber (f[Hz])	24.804	85.568	105.61
		m=4, n=1	
Carbon fiber (f[Hz])	31.595	184.26	243.88
Glass fiber (f[Hz])	19.929	105.40	148.91
Linoleum fiber (f[Hz])	19.700	103.47	141.42
		m=6, n=1	
Carbon fiber (f[Hz])	45.102	201.12	325.33
Glass fiber (f[Hz])	29.795	117.16	202.40
Linoleum fiber (f[Hz])	28.097	116.13	189.93

Table 6: Antisymmetric $0°/90°/0°/90°$ composite cylinder. First three frequencies in Hz for several thickness ratios and imposed half-wave numbers.

Mode	I	II	III
		R_α/h=1000	
		m=1, n=1	
Carbon fiber (f[Hz])	14.053	180.09	403.54
Glass fiber (f[Hz])	8.8111	111.21	224.06
Linoleum fiber (f[Hz])	8.7364	106.79	223.65
		m=2, n=2	
Carbon fiber (f[Hz])	14.694	359.41	777.58
Glass fiber (f[Hz])	9.2027	221.64	432.25
Linoleum fiber (f[Hz])	9.1298	212.79	431.40
		m=3, n=3	
Carbon fiber (f[Hz])	15.148	538.88	1158.0
Glass fiber (f[Hz])	9.4329	332.22	643.90
Linoleum fiber (f[Hz])	9.3703	318.95	642.60
		R_α/h=100	
		m=1, n=1	
Carbon fiber (f[Hz])	14.450	180.09	403.50
Glass fiber (f[Hz])	8.9990	111.21	224.05
Linoleum fiber (f[Hz])	8.9339	106.79	223.64
		m=2, n=2	
Carbon fiber (f[Hz])	21.207	359.38	777.33
Glass fiber (f[Hz])	12.380	221.64	432.21
Linoleum fiber (f[Hz])	12.473	212.79	431.31
		m=3, n=3	
Carbon fiber (f[Hz])	38.149	538.78	1157.2
Glass fiber (f[Hz])	21.217	332.21	643.77
Linoleum fiber (f[Hz])	21.640	318.93	642.32
		R_α/h=10	
		m=1, n=1	
Carbon fiber (f[Hz])	33.367	179.77	399.20
Glass fiber (f[Hz])	19.519	111.22	222.98
Linoleum fiber (f[Hz])	19.582	106.75	221.94
		m=2, n=2	
Carbon fiber (f[Hz])	110.90	356.29	748.83
Glass fiber (f[Hz])	69.566	221.43	427.18
Linoleum fiber (f[Hz])	68.581	212.10	421.11
		m=3, n=3	
Carbon fiber (f[Hz])	202.43	528.08	1008.1
Glass fiber (f[Hz])	135.34	331.33	628.39
Linoleum fiber (f[Hz])	130.74	316.35	606.90
		R_α/h=5	
		m=1, n=1	
Carbon fiber (f[Hz])	50.249	178.74	383.51
Glass fiber (f[Hz])	31.783	111.22	219.24
Linoleum fiber (f[Hz])	31.134	106.60	215.94
		m=2, n=2	
Carbon fiber (f[Hz])	145.12	346.93	534.38
Glass fiber (f[Hz])	100.72	220.70	401.35
Linoleum fiber (f[Hz])	95.885	209.87	369.54
		m=3, n=3	
Carbon fiber (f[Hz])	244.94	498.13	609.94
Glass fiber (f[Hz])	174.79	328.55	460.07
Linoleum fiber (f[Hz])	164.61	308.56	417.59

Table 7: Symmetric $0°/90°/0°$ composite cylindrical shell panel. First three frequencies in Hz for several thickness ratios and imposed half-wave numbers.

Mode	I	II	III
		R_α/h=1000	
		m=1, n=1	
Carbon fiber (f[Hz])	14.730	201.91	357.90
Glass fiber (f[Hz])	9.0282	117.20	209.96
Linoleum fiber (f[Hz])	9.1771	116.44	201.59
		m=2, n=2	
Carbon fiber (f[Hz])	15.359	402.97	690.15
Glass fiber (f[Hz])	9.4217	233.46	405.41
Linoleum fiber (f[Hz])	9.5717	231.95	389.33
		m=3, n=3	
Carbon fiber (f[Hz])	15.668	604.18	1028.0
Glass fiber (f[Hz])	9.6210	349.91	604.02
Linoleum fiber (f[Hz])	9.7560	347.63	580.09
		R_α/h=100	
		m=1, n=1	
Carbon fiber (f[Hz])	14.994	201.94	357.61
Glass fiber (f[Hz])	9.1943	117.20	209.87
Linoleum fiber (f[Hz])	9.3305	116.44	201.47
		m=2, n=2	
Carbon fiber (f[Hz])	19.239	402.98	689.29
Glass fiber (f[Hz])	11.907	233.46	405.18
Linoleum fiber (f[Hz])	11.749	231.93	388.99
		m=3, n=3	
Carbon fiber (f[Hz])	30.636	604.12	1026.1
Glass fiber (f[Hz])	19.138	349.88	603.62
Linoleum fiber (f[Hz])	18.253	347.58	579.42
		R_α/h=10	
		m=1, n=1	
Carbon fiber (f[Hz])	28.709	201.84	349.24
Glass fiber (f[Hz])	18.097	117.18	207.87
Linoleum fiber (f[Hz])	17.340	116.35	198.43
		m=2, n=2	
Carbon fiber (f[Hz])	94.938	400.11	646.10
Glass fiber (f[Hz])	63.561	233.12	397.53
Linoleum fiber (f[Hz])	59.147	230.95	374.81
		m=3, n=3	
Carbon fiber (f[Hz])	180.19	593.46	902.67
Glass fiber (f[Hz])	126.26	348.76	583.40
Linoleum fiber (f[Hz])	116.48	344.37	539.17
		R_α/h=5	
		m=1, n=1	
Carbon fiber (f[Hz])	45.102	201.12	325.33
Glass fiber (f[Hz])	29.795	117.16	202.40
Linoleum fiber (f[Hz])	28.097	116.13	189.93
		m=2, n=2	
Carbon fiber (f[Hz])	134.75	391.69	538.27
Glass fiber (f[Hz])	96.563	232.44	372.69
Linoleum fiber (f[Hz])	89.188	228.61	334.08
		m=3, n=3	
Carbon fiber (f[Hz])	231.08	564.82	679.29
Glass fiber (f[Hz])	170.56	346.40	485.07
Linoleum fiber (f[Hz])	156.62	336.60	438.85

Table 8: Antisymmetric 0°/90°/0°/90° composite cylindrical shell panel. First three frequencies in Hz for several thickness ratios and imposed half-wave numbers.

Mode	I	II	III
		R_α/h=1000	
		m=1, n=1	
Carbon fiber (f[Hz])	58.802	299.39	423.07
Glass fiber (f[Hz])	36.617	176.39	247.93
Linoleum fiber (f[Hz])	37.625	167.91	240.88
		m=2, n=2	
Carbon fiber (f[Hz])	62.131	593.17	808.68
Glass fiber (f[Hz])	38.692	352.03	470.45
Linoleum fiber (f[Hz])	39.594	334.27	460.07
		m=3, n=3	
Carbon fiber (f[Hz])	62.897	887.85	1202.8
Glass fiber (f[Hz])	39.166	527.78	698.58
Linoleum fiber (f[Hz])	40.037	500.88	684.14
		R_α/h=100	
		m=1, n=1	
Carbon fiber (f[Hz])	58.918	299.35	423.02
Glass fiber (f[Hz])	36.688	176.39	247.91
Linoleum fiber (f[Hz])	37.688	167.90	240.86
		m=2, n=2	
Carbon fiber (f[Hz])	64.472	592.90	808.42
Glass fiber (f[Hz])	40.100	352.00	470.38
Linoleum fiber (f[Hz])	40.856	334.20	459.97
		m=3, n=3	
Carbon fiber (f[Hz])	74.327	886.97	1202.0
Glass fiber (f[Hz])	46.081	527.69	698.42
Linoleum fiber (f[Hz])	46.282	500.66	683.82
		R_α/h=10	
		m=1, n=1	
Carbon fiber (f[Hz])	67.660	295.15	417.70
Glass fiber (f[Hz])	42.523	175.71	246.16
Linoleum fiber (f[Hz])	42.810	166.67	238.51
		m=2, n=2	
Carbon fiber (f[Hz])	139.95	565.85	776.92
Glass fiber (f[Hz])	95.147	349.01	463.50
Linoleum fiber (f[Hz])	89.812	327.17	447.72
		m=3, n=3	
Carbon fiber (f[Hz])	243.05	804.04	1070.7
Glass fiber (f[Hz])	174.86	519.34	678.53
Linoleum fiber (f[Hz])	161.00	479.30	642.36
		R_α/h=5	
		m=1, n=1	
Carbon fiber (f[Hz])	79.829	281.98	397.86
Glass fiber (f[Hz])	52.570	173.45	239.94
Linoleum fiber (f[Hz])	51.345	162.75	230.16
		m=2, n=2	
Carbon fiber (f[Hz])	180.55	490.97	602.97
Glass fiber (f[Hz])	131.77	338.51	434.19
Linoleum fiber (f[Hz])	121.26	305.40	392.46
		m=3, n=3	
Carbon fiber (f[Hz])	300.19	638.50	707.13
Glass fiber (f[Hz])	223.48	491.20	579.09
Linoleum fiber (f[Hz])	204.15	421.27	472.75

Table 9: Symmetric $0°/90°/0°$ composite spherical shell panel. First three frequencies in Hz for several thickness ratios and imposed half-wave numbers.

Mode	I	II	III
		R_α/h=1000	
		m=1, n=1	
Carbon fiber (f[Hz])	59.101	325.97	402.91
Glass fiber (f[Hz])	36.670	180.17	245.19
Linoleum fiber (f[Hz])	37.812	177.77	233.67
		m=2, n=2	
Carbon fiber (f[Hz])	62.514	651.94.	762.07
Glass fiber (f[Hz])	38.760	360.34	464.11
Linoleum fiber (f[Hz])	39.827	355.54	443.82
		m=3, n=3	
Carbon fiber (f[Hz])	63.286	977.90	1130.8
Glass fiber (f[Hz])	39.235	540.50	688.78
Linoleum fiber (f[Hz])	40.275	533.30	659.16
		R_α/h=100	
		m=1, n=1	
Carbon fiber (f[Hz])	59.203	325.93	402.85
Glass fiber (f[Hz])	36.738	180.16	245.17
Linoleum fiber (f[Hz])	37.869	177.75	233.65
		m=2, n=2	
Carbon fiber (f[Hz])	64.581	651.66	761.73
Glass fiber (f[Hz])	40.120	360.31	464.04
Linoleum fiber (f[Hz])	40.977	355.46	443.70
		m=3, n=3	
Carbon fiber (f[Hz])	73.502	977.02	1129.7
Glass fiber (f[Hz])	45.936	540.42	688.60
Linoleum fiber (f[Hz])	46.009	533.08	658.79
		R_α/h=10	
		m=1, n=1	
Carbon fiber (f[Hz])	67.320	321.51	396.66
Glass fiber (f[Hz])	42.425	179.43	243.37
Linoleum fiber (f[Hz])	42.647	176.42	231.13
		m=2, n=2	
Carbon fiber (f[Hz])	139.87	624.42	725.23
Glass fiber (f[Hz])	94.772	357.16	456.80
Linoleum fiber (f[Hz])	89.084	348.25	430.38
		m=3, n=3	
Carbon fiber (f[Hz])	245.50	895.49	1013.2
Glass fiber (f[Hz])	174.87	532.00	667.38
Linoleum fiber (f[Hz])	161.31	512.19	616.09
		R_α/h=5	
		m=1, n=1	
Carbon fiber (f[Hz])	79.947	307.53	377.18
Glass fiber (f[Hz])	52.460	177.05	237.13
Linoleum fiber (f[Hz])	51.184	172.23	222.75
		m=2, n=2	
Carbon fiber (f[Hz])	182.28	547.60	637.99
Glass fiber (f[Hz])	132.02	346.97	430.67
Linoleum fiber (f[Hz])	122.03	327.01	389.46
		m=3, n=3	
Carbon fiber (f[Hz])	300.39	719.40	728.94
Glass fiber (f[Hz])	223.91	506.62	597.41
Linoleum fiber (f[Hz])	205.14	457.57	489.57

Table 10: Antisymmetric $0°/90°/0°/90°$ composite spherical shell panel. First three frequencies in Hz for several thickness ratios and imposed half-wave numbers.

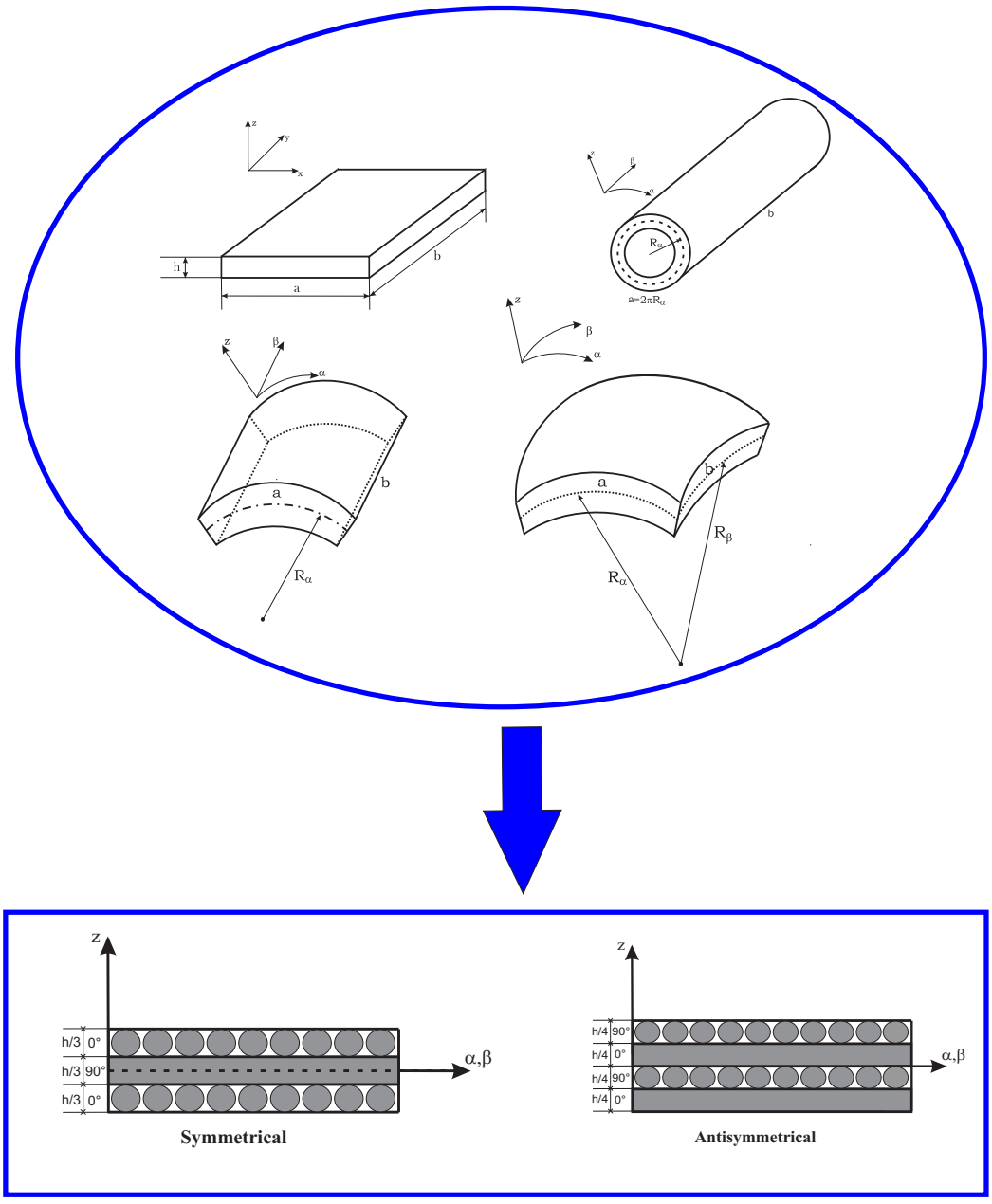

Figure 1: Geometries and symmetrical vs. antisymmetrical composite configurations.

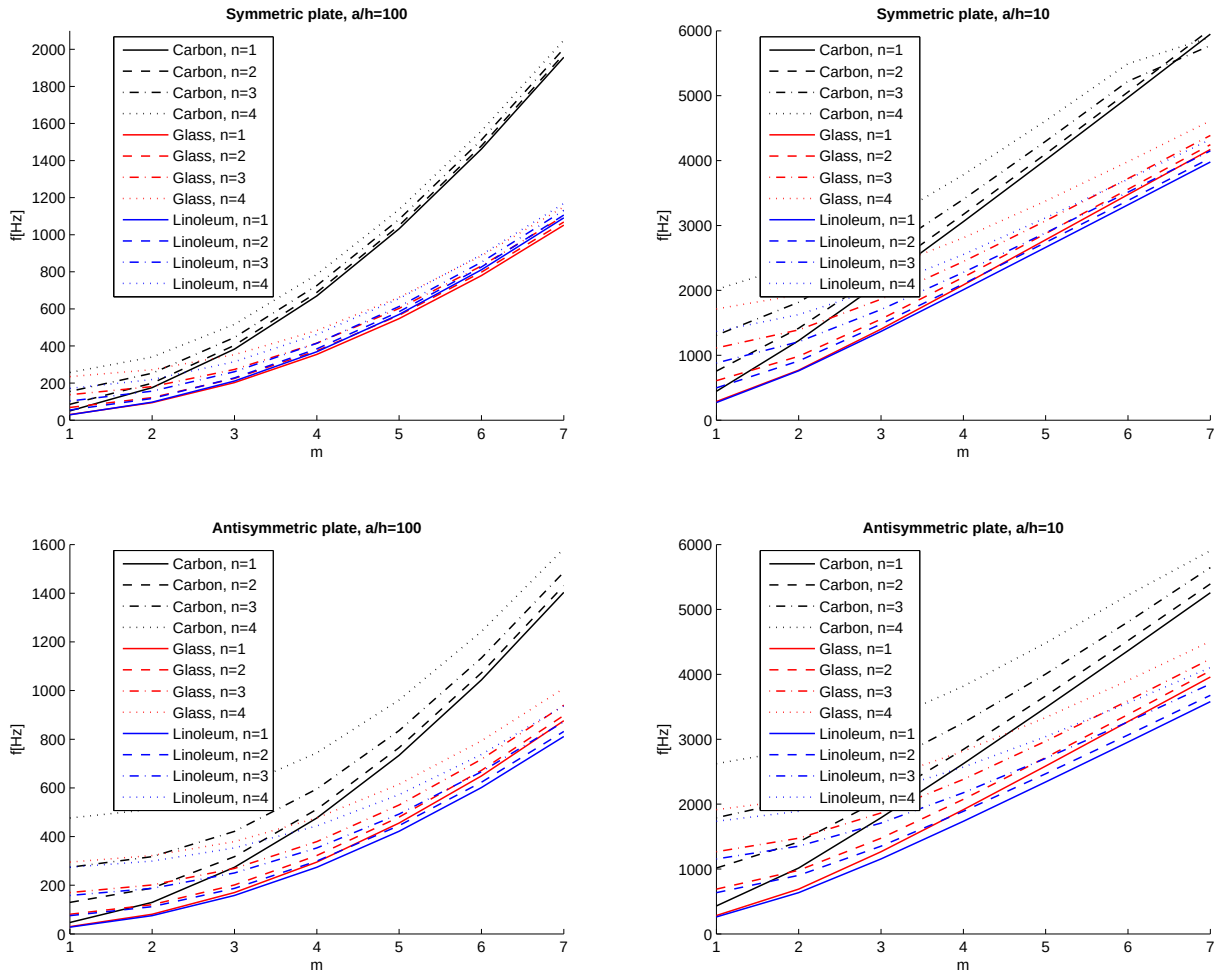

Figure 2: Symmetric and antisymmetric composite thin and thick plates. Frequency f[Hz] vs. half-wave numbers (m,n).

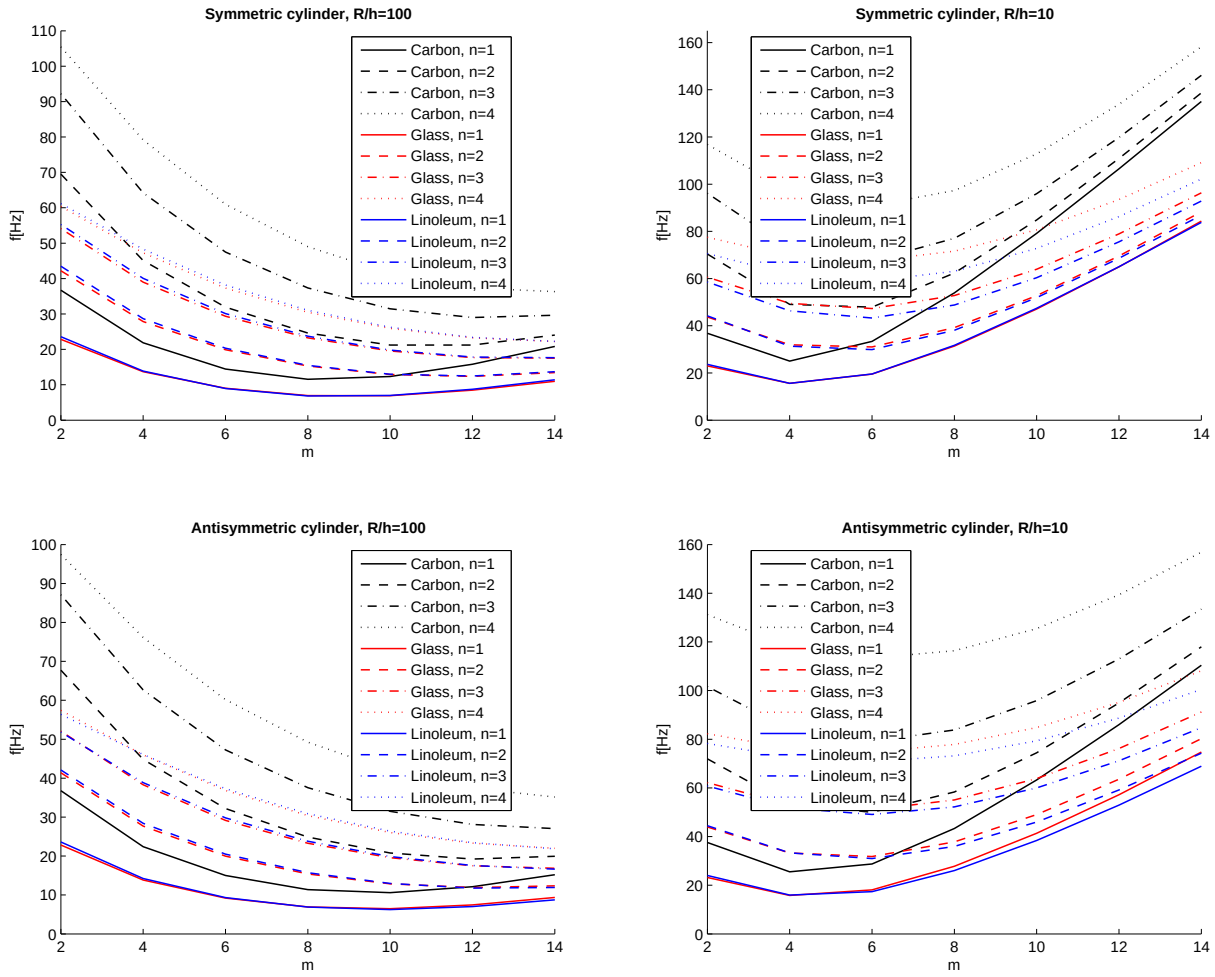

Figure 3: Symmetric and antisymmetric composite thin and thick cylinders. Frequency f[Hz] vs. half-wave numbers (m,n).

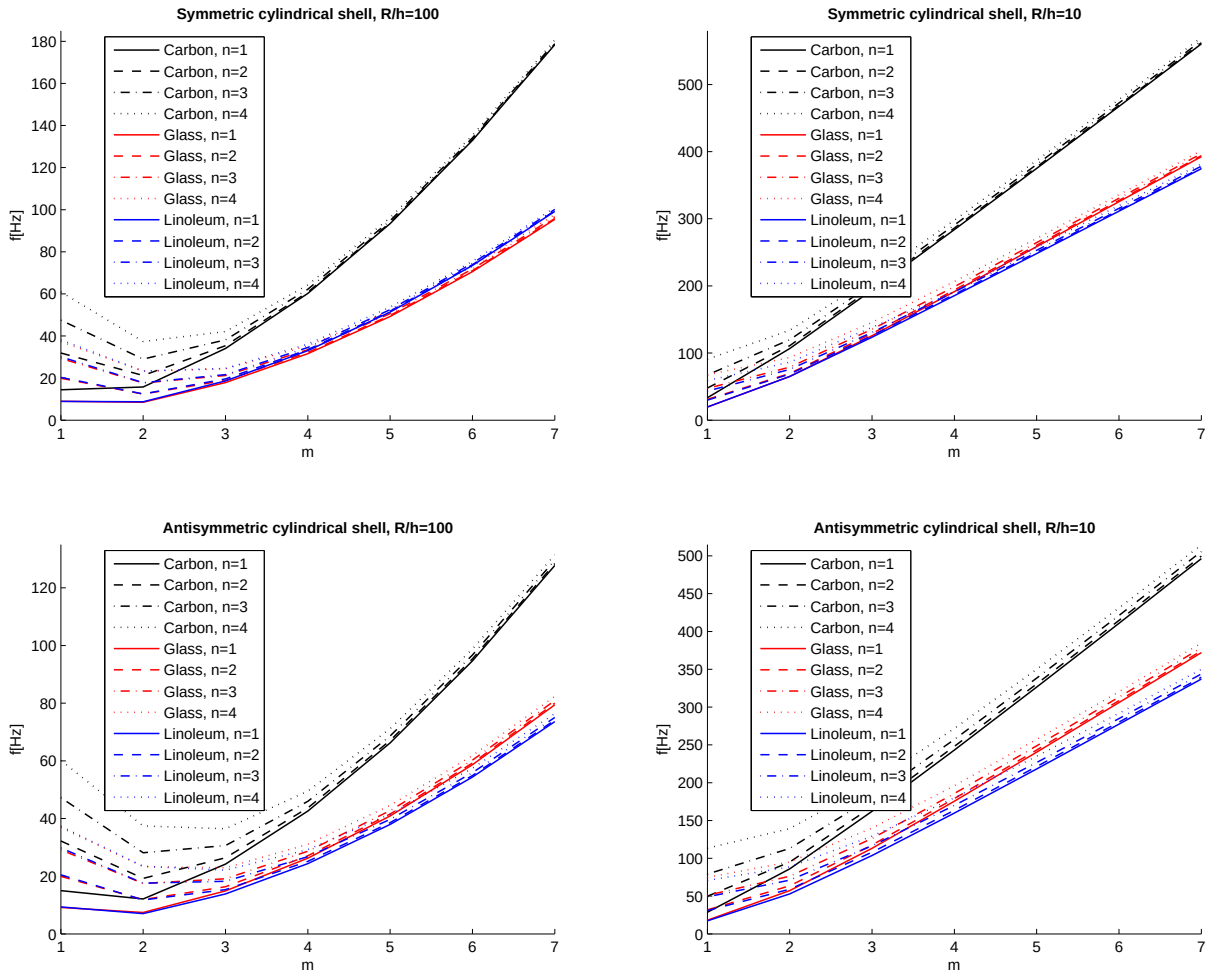

Figure 4: Symmetric and antisymmetric composite thin and thick cylindrical shell panels. Frequency f[Hz] vs. half-wave numbers (m,n).

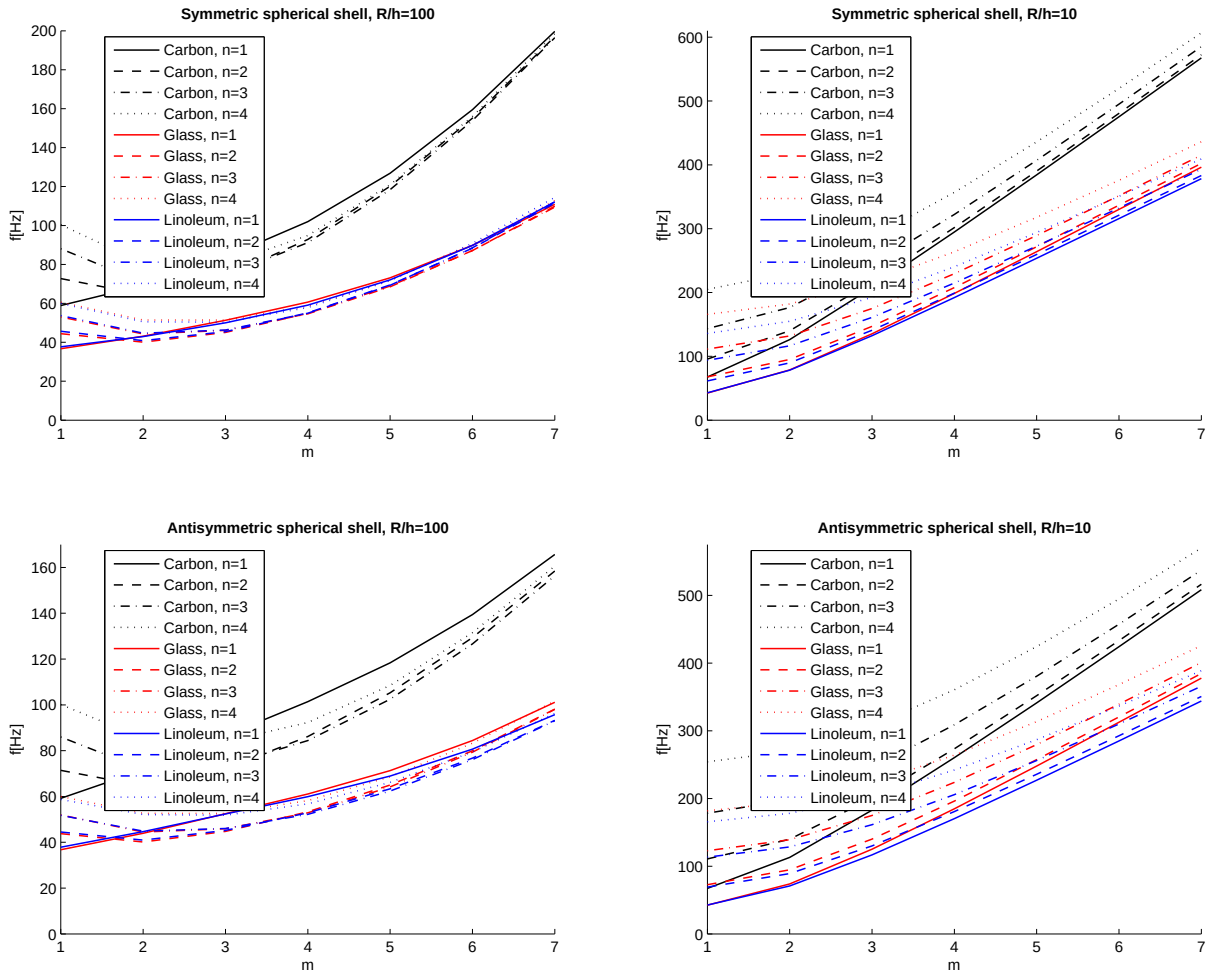

Figure 5: Symmetric and antisymmetric composite thin and thick spherical shell panels. Frequency f[Hz] vs. half-wave numbers (m,n).